

Figure Outline for Computational Perovskite Alloys Dataset

Panayotis Manganaris¹

Mannodi Group - Purdue MSE

January 27, 2022

Outline

1 Methodology

2 Results

3 reference

DFT simulation premise I

Perovskite structure summary

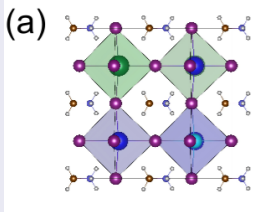


Figure: ABX_3 Cubic Perovskite Structure

Perovskite Chemical Domain

Table: ABX_3 Chemical Domain

A-site	B-site	X-site
MA	Pb	I
FA	Sn	Br
Cs	Ge	Cl
Rb	Ba	
K	Sr	
	Ca	
	Be	
	Mg	
	Si	
	V	
	Cr	
	Mn	
	Fe	
	Ni	
	Zn	
	Pd	

Composition Space Sampling I

construction of simulations

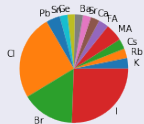
Table: Mix Table

cell construct	trials
2x2x2 Supercell A-site mixed	126
2x2x2 B & X-site mixed	5
2x2x2 Supercell B-site mixed	151
3x3x3 Supercell B-site mixed	5
4x4x4 Supercell B-site mixed	10
Alternative B-site elements	36
2x2x2 Pure	90
2x2x2 X-site mixed	127

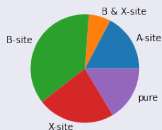
Composition Space Sampling II

Sampling in DFT dataset

constituent weight fractions out of whole



Representation of Alloy Constructs



Constituent Element Representation Fractions

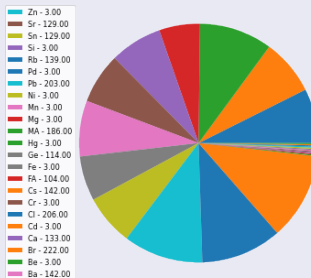


Figure: Species by weight and frequency, and alloy representations in DFT dataset

Composition Space Sampling III

Sampling in experimental dataset

data sourced from [1].

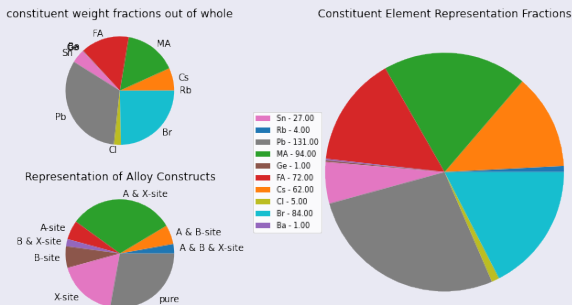


Figure: Species by weight and frequency, and alloy representations in experimental dataset to date

Topology of Computational Composition Space I

PCA projection of Mannodi compositions

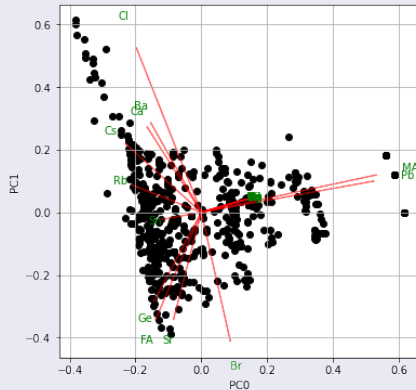


Figure: Definite Prismatic Topology in the Chemical Sample

Topology of Computational Composition Space II

computation samples Variance shares

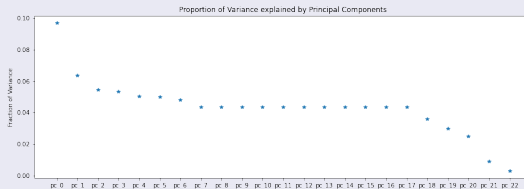


Figure: Variance in chemical ratios is fairly evenly spread. So, we expect little domain bias in future model training.

Topology of Experimental Composition Space I

projection of Experimental compositions into Mannodi space

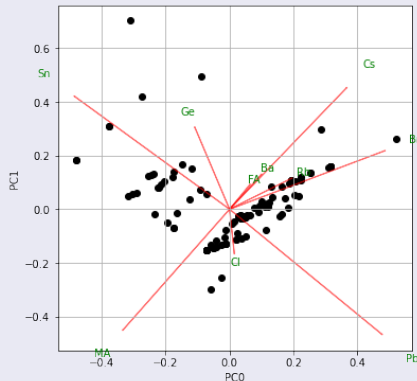


Figure: experimental data currently covers only boundaries of experimental domain. Alloying is more thoroughly explored in experimental domain.

Topology of Experimental Composition Space II

Experimental samples Variance shares

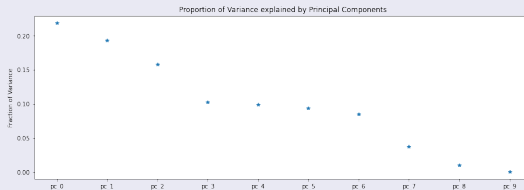


Figure: Variance in chemical ratios remains even.

Computational vs Experimental I

Band Gaps

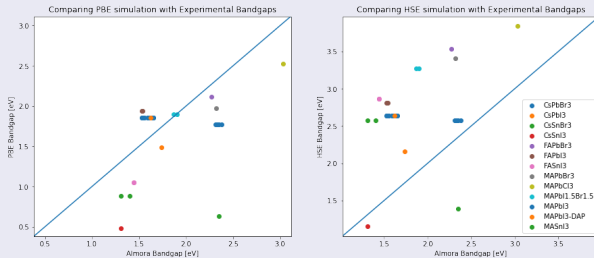


Figure: HSE and PBE bandgaps vs experimental measures show clearly computation methods need improvement

Trends in Computational Data I

LC vs Bg in HSE results

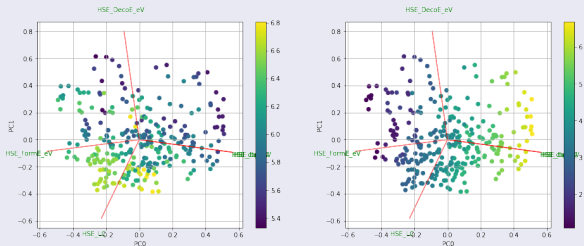


Figure: In this projection larger lattice constants appear to inversely correlate with larger band gaps

Trends in Computational Data II

SLME vs Bg in PBE results

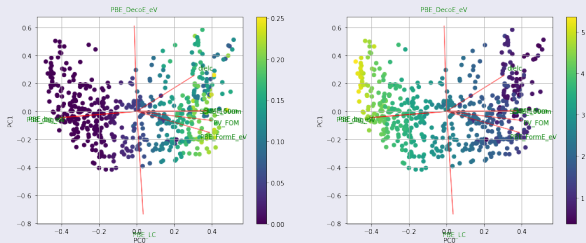


Figure: In this projection larger band gaps appear to inversely correlate with higher SLME values recorded for 5um absorption layers

citations



Osbel Almora, Derya Baran, Guillermo C. Bazan, Christian Berger, Carlos I. Cabrera, Kylie R. Catchpole, Sule ErtenEla, Fei Guo, Jens Hauch, Anita W. Y. HoBaillie, T. Jesper Jacobsson, Rene A. J. Janssen, Thomas Kirchartz, Nikos Kopidakis, Yongfang Li, Maria A. Loi, Richard R. Lunt, Xavier Mathew, Michael D. McGehee, Jie Min, David B. Mitzi, Mohammad K. Nazeeruddin, Jenny Nelson, Ana F. Nogueira, Ulrich W. Paetzold, NamGyu Park, Barry P. Rand, Uwe Rau, Henry J. Snaith, Eva Unger, Lídice VaillantRoca, HinLap Yip, and Christoph J. Brabec.
Device performance of emerging photovoltaic materials (version 1).
Advanced Energy Materials, 11(11):2002774, 2020.